

A cost-effective pH-sensitive release system for environment detection

Zhaoliang Zheng,^{a,b} Xing Huang^c and Dmitry Shchukin^b

Supplementary Information

1. Material and Reagents

Tetraethyl orthosilicate (reagent grade, 98%), sodium hydroxide solution (~1.0 M NaOH), hexadecyltrimethylammonium bromide ($\geq 98\%$), toluene (anhydrous, 99.8%), calcein, cobalt(II) nitrate hexahydrate (ACS reagent, $\geq 98\%$), and sodium carbonate ($> 99.95\%$ dry basis) were all purchased from Sigma-Aldrich. (Trimethoxysilylpropyl)-ethylenediamine triacetic acid trisodium salt (45% in water) was bought from ABCR GmbH & CO. KG. **The buffer solutions were got from Carl ROTH.**

2. Synthetic procedure

MCM-41 nanoparticles: the silica mesoporous nanoparticles were fabricated according to a previously reported method¹. Briefly, 950 mL of deionized water, 2 g of hexadecyltrimethylammonium bromide and 14 mL of sodium hydroxide solution (~1.0 M NaOH) were mixed and preheated at 80 °C for 1 h. Then 10 mL of TEOS was dropped in within 30 min. The mixture was further heated for 2 hours and followed by natural cooling down. The template can be removed by calcination at 550 °C.

Ethylenediamine triacetate functionalized silica MCM-41 nanocontainers: The bared mesoporous silica solid (2 g) was suspended in 500 mL of dry toluene to which 0.14 mL of (trimethoxysilylpropyl)-ethylenediamine triacetic acid trisodium salt aqueous solution (45% in water) was added. The mixed solution was continuously stirred at 120 °C for 20 h, resulting in MCM-41 functionalized with ethylenediamine triacetic acid.

Diethylenetriamine functionalized silica MCM-41 nanocontainers: The bared mesoporous silica solid (2 g) was suspended in 500 mL of dry toluene to which 0.04 mL (for 0.2 mmol/g) of N-(3-trimethoxysilylpropyl)diethylenetriamine) was added. The mixed solution was continuously stirred at 120 °C for 20 h, resulting in MCM-41 functionalized with en-type agent.

ethylenediamine-4-oxo-2-butenic functionalized silica MCM-41 nanocontainers: The bared mesoporous silica solid (2 g) was suspended in 500 mL of dry toluene to which 0.05 mL (for 0.2 mmol/g) of N-[3-(Trimethoxysilyl)propyl]ethylenediamine was added. The mixed solution was continuously stirred at 120 °C for 20 h. 2 g of the resulting solid was suspended in 50 mL of DMSO to which 43 μ L of triethylamine and 200 mg (for 0.2 mmol/g) of succinic anhydride were added. The mixed solution was

continuously stirred at 40 °C for 48 h, resulting in ethylenediamine-4-oxo-2-butenic functionalized silica MCM-41 nanocontainers.

Loading procedure: The subsequent loading of the containers with cargo molecules was conducted under reduced pressure (30 mbar) for three times. The as-loaded containers were separated by filtration and further cleaned by method developed by us². To obtain “clean” loaded nanocontainers without surface absorbed calcein, a quick washing method was developed to prevent spontaneous leakage of the loaded active compounds to the maximum extent. A home-made washing machine was simply composed of a piece of filter paper with a transparency of 0.05 μm , a funnel and a pump. Before washing, a thin layer of pristine solid was carefully deposited on the filter paper. Then water was added on the solid droplet. The procedure was cycled for several times till the released amount of calcein (determined by fluorescence) remained constant.

Synthetic procedure and scaling up strategy. A sprayer was used for forming nanovalves on the loaded containers in a large amount. Typically, 0.1 M $\text{Co}(\text{NO}_3)_2$ solution was sprayed on loaded containers, followed by removing salt excess. The same amount of 0.2 M Na_2CO_3 solution was then sprayed. The resulting product was sealed for 3-days aging and then mixed with aluminum oxides powder for environmental detection.

Formation of Precipitates. For the process of forming precipitates, we injected 5 mL of Na_2CO_3 solution quickly into the tube containing 5 mL of 0.1 M $\text{Co}(\text{NO}_3)_2$ solution to check whether the product was stable enough to cease the notable precipitation. After the formation of gelatinous precipitates, the previous salt solutions suddenly lose their fluidity and transparency. Aging was conducted with sealed tube under atmospheric pressure and at room temperature.

pH detection. A drop (about 0.02 mL) of solution was dropped onto the surface of the tablet or immersing the tablets in to aqueous solution under a UV lamp (326 nm). The process was recorded with a camera.

3. Characterization

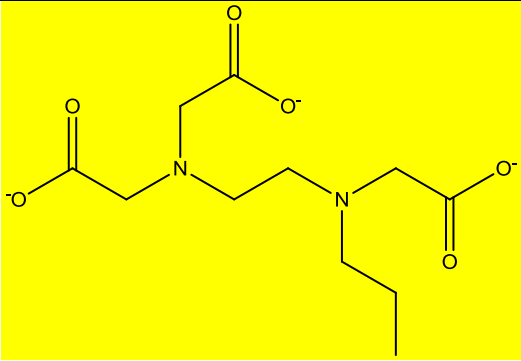
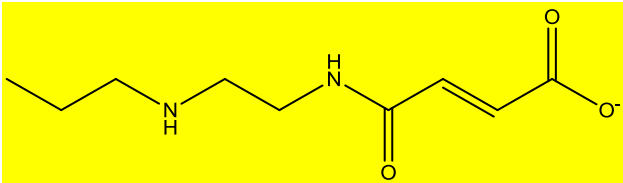
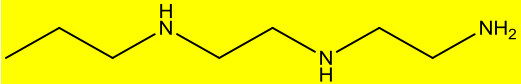
HADDF STEM image and STEM EDX mapping were recorded from Cs-corrected Titan 80–300 microscopes operated at 300 kV. Structure and porosity of the solid samples were characterized by BET (Macromeritics TriStar 3000 system), DLS (Malvern Zetasizer 4 and SAXS (a Nonius rotating anode (Cu $K\alpha$ radiation, $\lambda = 1.5406 \text{ \AA}$) with pinhole collimation and a MAR CCD area detector (sample-detector distance of 740 mm). SAXS measurements were also conducted with transition metal precipitates in a capillary (1.5 mm in diameter, Borokapillaren, GLAS), to investigate the porous structure. SAXS profiles were recorded under vacuum on a Nanostar instrument (Bruker AXS) using Cu-K α radiation with a wavelength of $\lambda = 0.154 \text{ nm}$. A single photon counting area detector (HiStar, Bruker AXS) was used at a sample-detector distance of 25.2 cm and a range of scattering vector q from 0.035 to 0.7 nm^{-1} was covered. The capillaries stood vertically during aging for 3 days. During measurement they were horizontal. Thermogravimetric analysis (TGA) was performed on a Netzsch TG 209 F1 at a scanning rate of 20 K/min under a nitrogen atmosphere. Aqueous suspensions containing 1 mL of precipitate and 4 mL of water were titrated against HCl standard solution with $\text{pH} = 1$ by using a Metrohm Autotitrator. Titration allowed for determination of approximate pH and ERC ranges in which the precipitates react with acid. The pH values were measured by a pH meter (HI9124, Hanna).

UV-vis spectroscopy (8453 UV-visible spectrophotometer, Agilent technologies) and fluorescence spectroscopy (FluoroMax-4, Horiba) were applied to determine the release profile of calcein². The 1 mg of sample powder was placed in the bottom of a small bag which is made of a screen mesh membrane

with mesh size around 1 μm . Then, the buffer solution (at $\text{pH} \approx 7$, 4 mL) was added to the cuvette till the bottom of the bag was immersed into water. A 5-mm stirring bar was added to the cuvette. The solution in the cuvette was stirred vigorously to quickly balance the concentration of the releasing calcein. The detection was focused into the solution at 2 cm above the bottom and around 1 cm below the top of the cuvette. Stimulated release from the containers was accomplished by changing the neutral solution with the one with lower pH values.

4. Supplementary Tables and Figures.

Table S1. Three types of functionalization and the Co content for each sample.

Functionalizing moiety	Structure	Co content (wt%)
N-propyl-ethylenediamine-N,N',N'-triacetate		1.7 ^a
		1.7 ^b
		1.5 ^c
		0.1 (trace) ^d
N-propyl-N'-ethylenediamine-4-oxo-2-butenoic acid		0.31 ^a
N-propyl-diethylenetriamine		1.0 ^a

^a Nanovalves are formed with $\text{Co}(\text{NO}_3)_2$ (0.1 M) and Na_2CO_3 (0.2 M) solutions. ^b 0.5 M and 1.0 M, ^c 1.0 M and 2.0 M, ^d 1 mM and 2 mM.

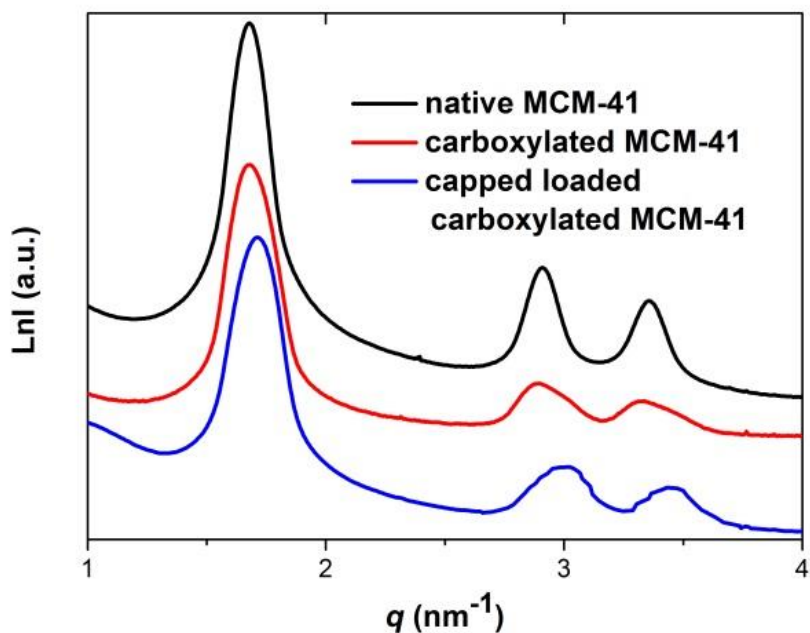


Figure S 1. SAXS spectra of native MCM-41, carboxylated MCM-41 and calcein-loaded carboxylated MCM-41 with nanovalves.

Fig. S1 shows small angle x-ray scattering (SAXS) curves of the three samples. All of them (native, carboxylate functionalized and capped loaded carboxylate functionalized silica nanocontainers) exhibit clear (100), (110) and (200) peaks at $q = 1.7, 2.9$ and 3.4 nm^{-1} , confirming a structure with hexagonal $p6mm$ order. Particularly for the two modified samples, the regular mesoporous structure can be roughly preserved because the (100) peak remains intact when compared with native MCM-41 and the other two at higher q values show no obvious weakening and broadening.

Table S2. Structural information of native MCM-41 obtained from DLS and N2 adsorption results.

ξ -size (nm)	ξ -potential (mV)	BET (m ² /g)	Pore volume (m ³ /g)	Pore size (nm)
154.6 ± 12.5	-20.2 ± 1.5	1075.5	0.93	3.8

0.1 M for cobalt salt solution was selected in our work because the higher concentration (e.g. 500 mM and 1 M) cannot lead to a higher Co content in capped loaded nanocontainers after the formation of nanovalves (Table S1). For the lower concentrations (1 mM), the SAXS result showed no evidence for the formation of 3D self-supporting porous structure but only single and scattered mass fractal state (Figure S). Furthermore, the premature leakage in neutral condition becomes notable (40% of loaded amount) as the concentration of spraying solution getting diluted.

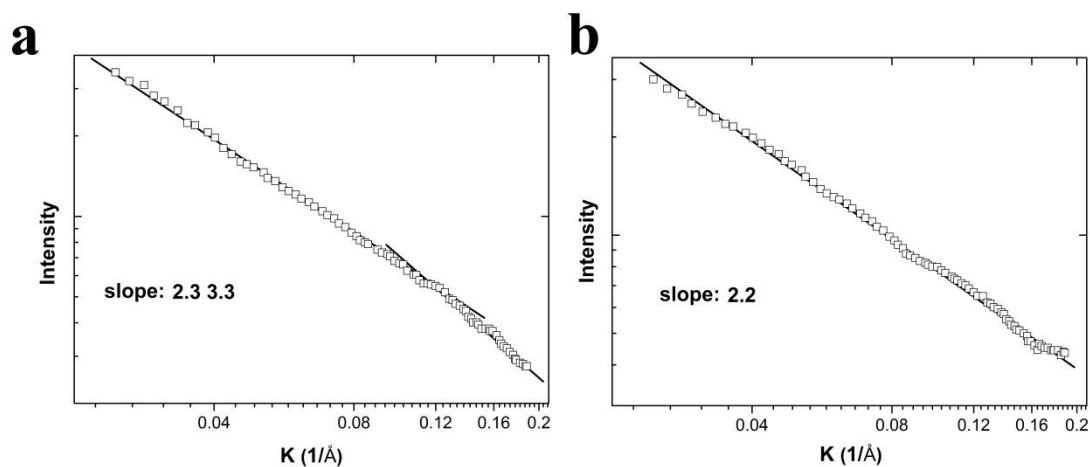


Fig. S2 (a) Porod plots and corresponding slopes of precipitates derived from $\text{Co}(\text{NO}_3)_2$ (0.1 M) and Na_2CO_3 (0.2 M) solutions after 10-days aging at room temperature. (b) Porod plots and corresponding slopes of precipitates derived from $\text{Co}(\text{NO}_3)_2$ (1 mM) and Na_2CO_3 (2 mM) solutions after 3-days aging at room temperature.

The power law information derived from the Porod region of scattering for GPs reveals fractal behavior. In the Porod region the scattered intensity decays as a power law: $I(K) \sim K^{-D}$. Fractal dimension, $D = -2d_f + d_s$ where D is obtained from the value of the slope at the Porod region, d_f is the mass fractal dimension ($0 \leq d_f \leq 3$) and d_s is the surface fractal dimension ($2 \leq d_s \leq 3$)³. The Guinier radius of the initial curvature of the SAXS curve can be obtained by the position of crossover, which is about $K = 0.047 \text{ \AA}^{-1}$. Thus the radius equals roughly 22 \AA .

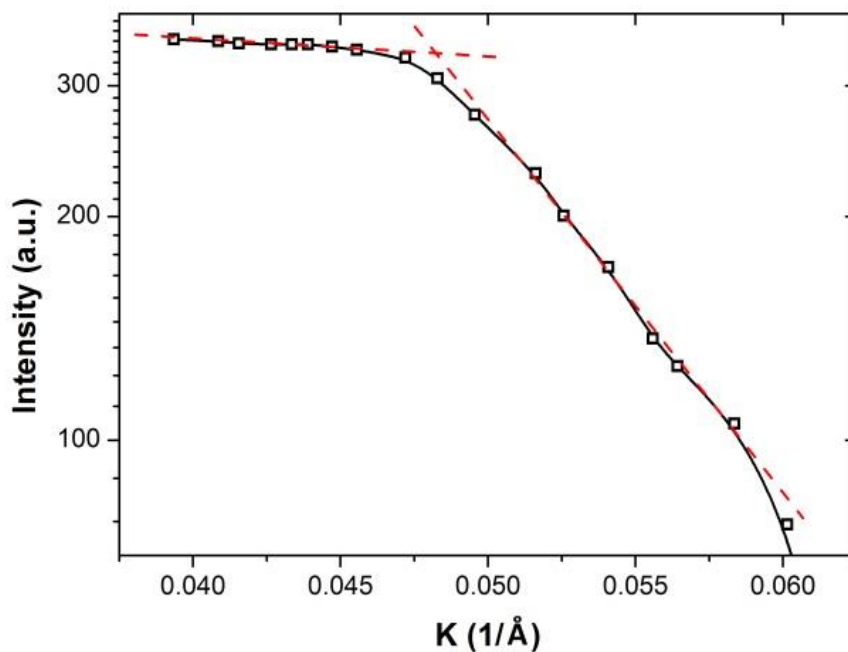


Figure S3. Guinier regime of SAXS spectra of cobalt basic carbonate precipitates. The Guinier radius of the initial curvature of the SAXS curve can be simply obtained by the position of crossover.

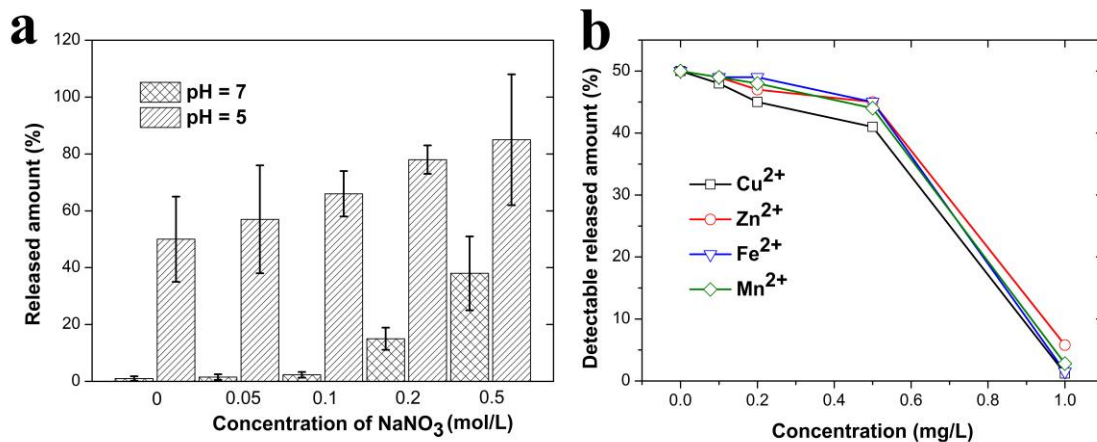


Fig. S4 (a) Released amount of loaded calcein from the capped nanocontainers with Co-Carbonate nanovalves in the period of 1000 min. Ionic strength in pH 7 and 5 have been tailored by addition of NaNO₃. (b) Detectable released amount of calcein as a function of concentration of transition metal ions (Cu²⁺, Zn²⁺, Fe²⁺ and Mn²⁺).

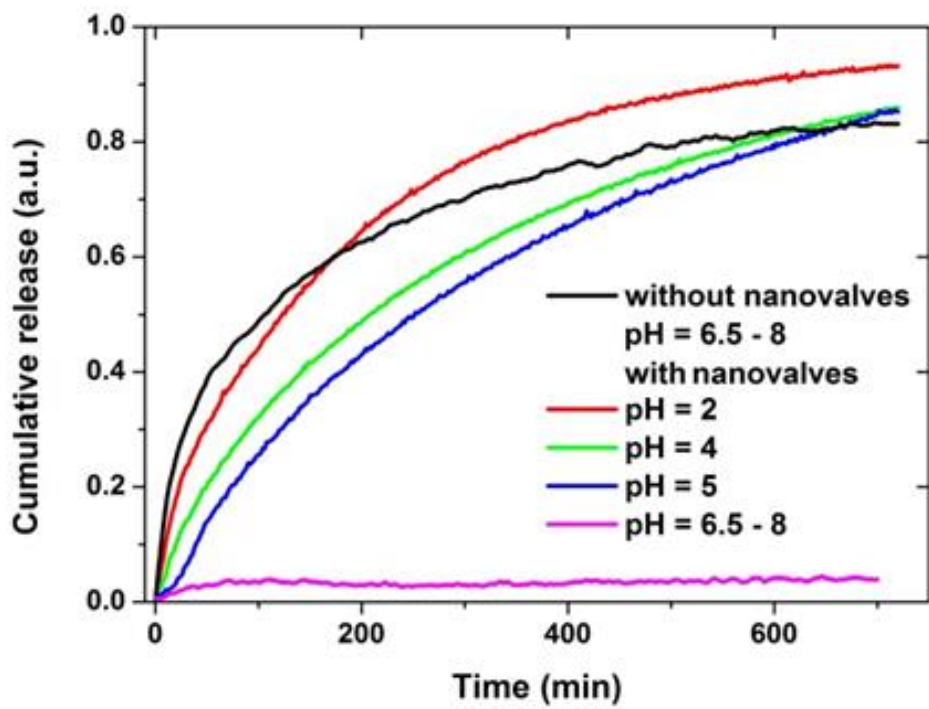


Figure S 5. pH sensitive release profile of BTA from the loaded nanocontainers with Co-Carbonate nanovalves.

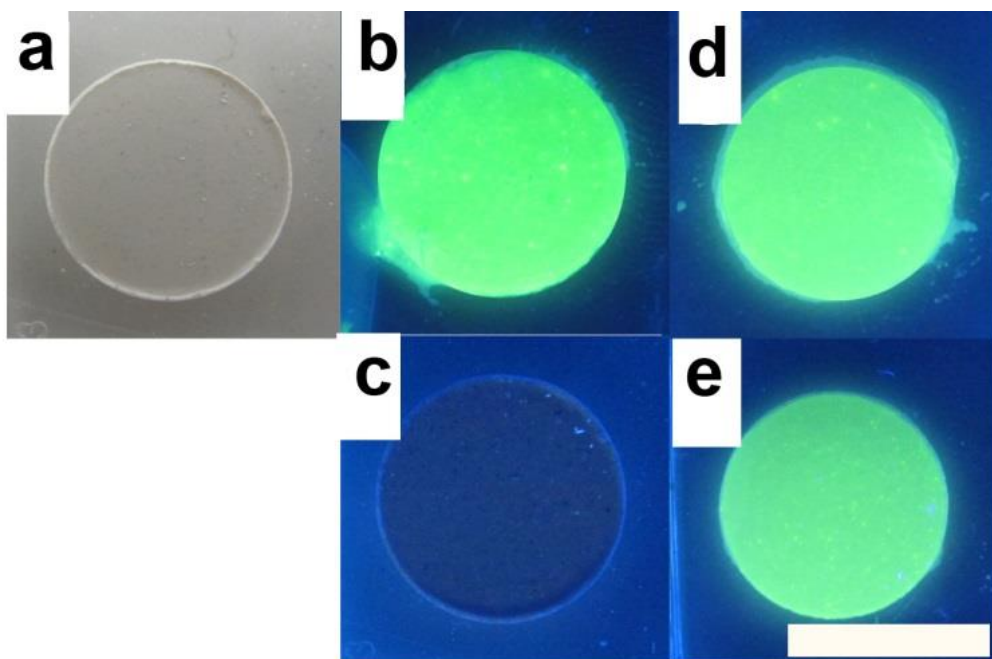


Figure S6. (a) Image of the tablet comprising containers with Co-Carbonate nanovalves and aluminum oxide. Under a UV lamp (326 nm), (b) the tablet without uncapped containers exhibits green colour immediately after immersion in water with a neutral pH, while (c) no emission can be observed for the tablet with uncapped containers in the same condition. (d) pH = 4 and (e) pH = 5 can lead the appearance of green colour at 10 s and 60 s, respectively.

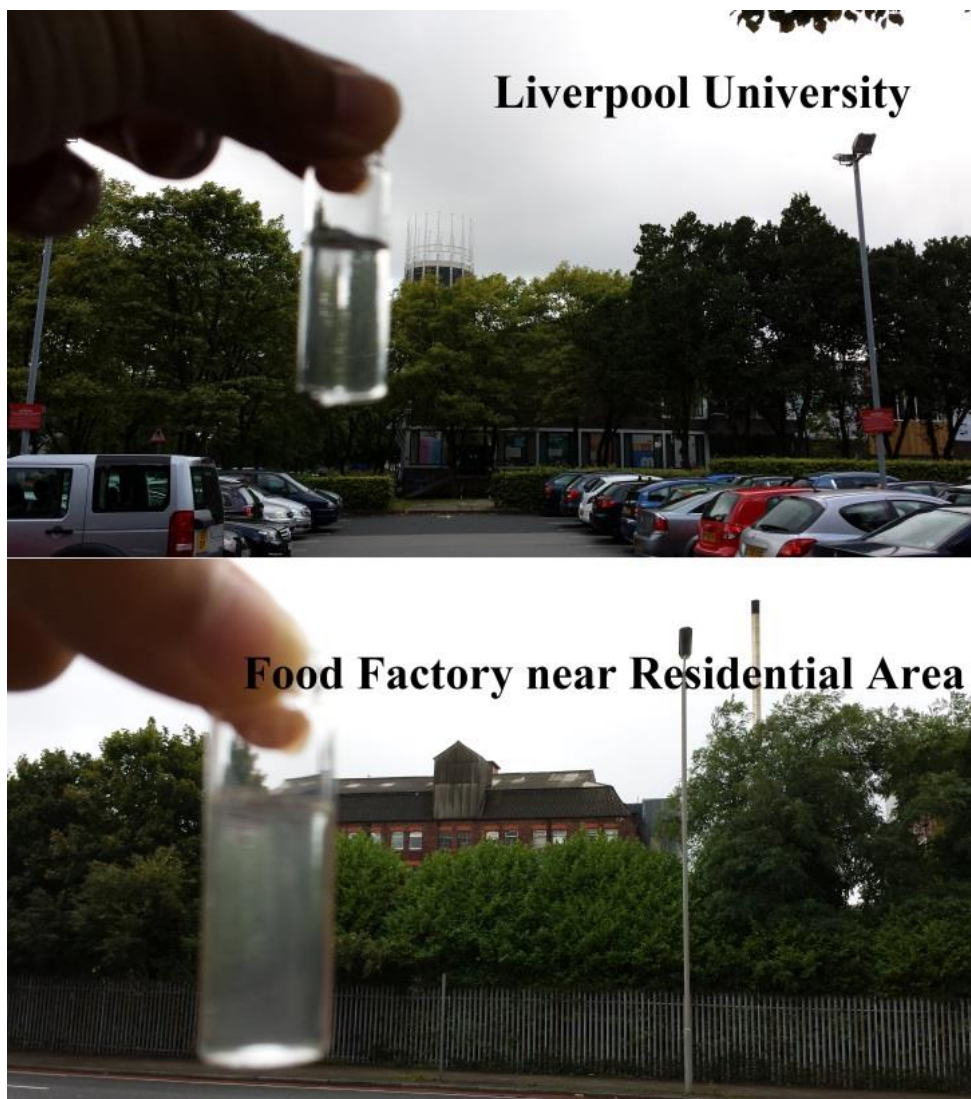


Fig. S7 The water samples collected from Liverpool University and food factory near residential area.

- 1 S. Angelos, N. M. Khashab, Y.-W. Yang, A. Trabolsi, H. A. Khatib, J. F. Stoddart and J. I. Zink, *J. Am. Chem. Soc.*, 2009, **131**, 12912.
- 2 Z. Zheng, X. Huang, M. Schenderlein, D. Borisova, R. Cao, H. Möhwald and D. Shchukin, *Adv. Func. Mater.*, 2013, **23**, 3307.
- 3 D. W. Schaefer, A. J. Hurd, D. K. Christen, S. Spooner and J. S. Lin, *MRS Online Proceedings Library*, 1988, **121**, 305.